

LM-02K058  
August 21, 2002

---

## **The Evolution of the Segregation Behavior of Alloying Elements in a Low-Alloy Steel**

A.J. Papworth, D.B. Knorr, D.B. Williams

---

### **NOTICE**

This report was prepared as an account of work sponsored by the United States Government. Neither the United States, nor the United States Department of Energy, nor any of their employees, nor any of their contractors, subcontractors, or their employees, makes any warranty, express or implied, or assumes any legal liability or responsibility for the accuracy, completeness or usefulness of any information, apparatus, product or process disclosed, or represents that its use would not infringe privately owned rights.

# THE EVOLUTION OF THE SEGREGATION BEHAVIOR OF ALLOYING ELEMENTS IN A LOW-ALLOY STEEL

Adam J. Papworth, David B. Knorr<sup>†</sup> and David B. Williams

Lehigh University, Materials Research Center, 5 East Packer Avenue, Bethlehem, PA 18015.

<sup>†</sup>Lockheed-Martin Corp., Schenectady, NY 12309.

## Keywords

Segregation, Grain Boundaries, Low Alloy Steel, Temper Embrittlement.

## INTRODUCTION

The segregation of alloying and impurity elements to prior austenite grain boundaries (PAGBs) in low-alloy steels [1] controls temper-embrittlement [2,3] although the precise microchemical and microstructural interactions are, as yet, unclear because of the many variables involved. Competing segregation and de-segregation phenomena are observed. For example, Auger analyses of fracture surfaces indicate that brittle fracture is caused by the segregation of P [4,5] to the PAGB. The addition of small amounts (~0.5 wt%) of Mo appears to retard, but not stop, temper-embrittlement [6,7], possibly due to Mo<sub>2</sub>C precipitates that form at elevated temperatures causing de-segregation of Mo from the PAGB [8,9]. The relationship between segregation and temper embrittlement is further complicated in commercial alloys by both the number of segregating elements and the complex, multi-stage heat treatments. Auger analysis pre-selects the most embrittled boundaries and so the complete distribution of segregants across all PAGBs cannot be determined by this technique. Previous work has shown how X-ray mapping (XRM) in a field-emission gun scanning transmission electron microscope (FEG-STEM) offers a more complete view of the distribution of segregants on both non-embrittled and embrittled PAGBs [10,11,12]. XRM was used to observe the evolution of the segregation and desegregation of five elements during four successive heat-treatment stages of commercial low-alloy steel forgings. In the last and crucial temper-embrittlement stage, increases in the degree and frequency of Ni segregation occur while other elements either segregate, remain constant or desegregate from the PAGBs.

## EXPERIMENTAL PROCEDURE

Two heats of a low-alloy steel (compositions given in Table 1 below) were given the following similar sequence of heat treatments: 1) both steels were normalized and air cooled, 2) steel #1 was austenitized at 857°C for 8.5 hours (steel #2 for 9 hours) and water quenched, 3) steel #1 was tempered at 632°C for 8 hours (steel #2 at 643°C for 15 hours) and fan cooled, 4) both steels were stress-relief annealed at 565°C for 50 hours, followed by a slow cool to room temperature at 11°C per hour, 5) steel #1 was temper embrittled at 427°C for 6 months (steel #2 for 9 months). The resultant microstructure is tempered lower bainite with a prior austenite grain size of ~40 µm.

Table 1 Compositions of Steels

Element (wt. %)	Ni	Cr	Mo	Mn	C	P	V
Steel #1 (balance Fe)	3.01	1.83	0.47	0.29	0.22	0.005	0.005
Steel #2 (balance Fe)	2.93	1.73	0.56	0.31	0.21	0.010	0.036

TEM specimens were made from samples taken after each of the above heat treatments by manual polishing of 3-mm discs to a thickness of  $\sim 40 \mu\text{m}$ . The discs were then ion-beam thinned at an angle of  $4^\circ$ , using a Gatan precision ion polishing system. The microstructural and microchemical analyses were carried out using a VG HB603 FEG-STEM with a probe size of 1.4 nm full width tenth maximum and a beam current of 0.5 nA. The FEG-STEM uses an Oxford windowless Si(Li) X-ray energy dispersive spectrometer with a 0.3 sr solid angle of detection. X-ray acquisition was carried out on an Oxford exl system, where elemental windows were defined in the experimental spectra for the  $K_\alpha$  lines of C, O, Al, Si, P, V, Cr, Mn, Fe, Ni, Cu, Mo and the  $L_\alpha$  line of Mo. Two normalizing backgrounds were defined from 3.3-3.8 keV and 10.0-12.0 keV respectively. At least 25 PAGBs were analyzed after each heat treatment. All showed segregation of one or more elements, except for the austenitized and quenched condition in which only about half the boundaries showed detectable segregation. All PAGBs were analyzed using two different methods: a) X-ray maps with an acquisition time of 100 ms/pixel with a resolution of 128x128 pixels, b) digital line-scans 64 nm in length containing 64 spectra/scan. Each spectrum in the line scan was acquired for 5 s, and was normalized with respect to the matrix characteristic intensity to remove any effects of thickness.

## RESULTS AND DISCUSSION

Following normalizing and air-cooling, the steels were reheated into the austenite regime, dissolving all but the largest precipitates, thereby leaving most of the alloying elements in solid solution after subsequent water quenching. Figure 1 is a set of X-ray maps of a PAGB segment, taken from such an austenitized and quenched specimen of steel #1. It is clear that most precipitates have indeed dissolved, but Mo and Cr have segregated to this PAGB. Similar sets of maps were acquired in the tempered, stress-relieved and temper-embrittled conditions for both steels and, based on the segregation information in these maps, digital line-scans were acquired for the elements Ni, Mn, Cr, Mo and the impurity element, P. (Note, e.g., in Figure 1 that V did not segregate, nor was it a strong segregant in any of the conditions). To give a pictorial overview of the segregation to all 25 boundaries mapped from each steel for a particular heat treatment, pie charts were constructed from the line scan data for each element. There are four fields in these pie charts: i) zero detectable segregation (i.e. segregation levels that did not meet the inequality  $I_p - I_B \geq 3(I_B)^{1/2}$ , where  $I_p$  is the peak intensity and  $I_B$  is the average X-ray intensity in the matrix from each element); ii) segregation levels that met the inequality  $I_p - I_B \geq 3(I_B)^{1/2}$ ; iii) segregation levels where  $I_p - I_B$  was 1.5 X that of  $I_B$ ; iv) segregation levels where  $I_p - I_B$  was 2.0 X that of  $I_B$ . In the case of P segregation, the amount of P dissolved in the matrix was less than the detection limit for P so  $I_B$  for P represents only bremsstrahlung intensity. For the Ni, Cr, Mo, Mn alloying elements, the matrix intensity  $I_B$  is the sum of the characteristic intensity plus the bremsstrahlung. The pie charts give a sense of both the magnitude (degree) of segregation of each element (denoted by the gray level) and the frequency of segregation to all PAGBs (denoted by the fractional coverage of the pie chart).

Figure 2 shows the pie charts for all four heat treatment conditions of the five segregating elements from steel #1 and for the last two conditions for steel #2. It can be seen that, for steel #1, in the austenitized and quenched condition, there is no detectable segregation of Ni or Mn and only a very small amount of P segregation, whereas  $\sim 50\%$  of the PAGBs have Mo and  $\sim 25\%$  have Cr segregation, similar to the maps in Figure 1. Note that the problems of the detection of P segregation in the presence of Mo, because of the overlapping P  $K_\alpha$  and Mo  $L_1$  peaks at 2013 eV, has been discussed elsewhere [13]. If there is a significant characteristic peak at 2013 eV, the results may be summarized as follows; the minimum amount of Mo detectable depends on the specimen thickness but is

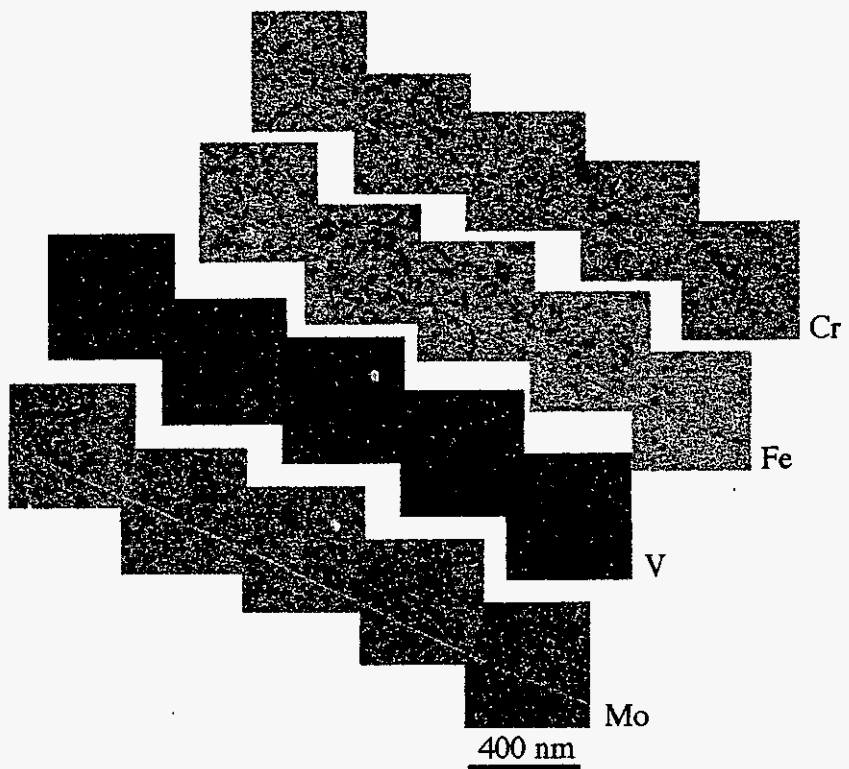


Figure 1. X-ray maps of a PAGB in steel #1 in the austenitized and quenched condition, showing Mo and Cr segregation and Fe depletion. A few small precipitates remain undissolved.

typically in the range 4.0-7.0 wt%. The minimum amount of P detectable in the absence of Mo depends on the specimen thickness but is generally in the range 0.08-0.14 wt%. If a significant peak is observed at 2013 eV, and if the amount of Mo is <4.0 wt%, which would be known from the Mo Ka peak, then there must be >0.08 – 0.14 wt% P present (depending on specimen thickness) within the interaction volume. Note that segregation to this extent represents a > 8x increase over the bulk concentration. Applying similar analyses to the quenched and tempered, stress-relieved, and the temper-embrittled conditions, the segregation behavior can be traced as the steel is processed.

The pie charts in the austenized and quenched sample were constructed from all the PAGBs that were analyzed. For example in steel #1, Mo, P and Cr were the only elements to have segregated in the austenized and quenched condition, as Cr and P were always found to co-segregate with Mo. The use of pie charts only from PAGBs showing segregation would imply that all PAGBs in the austenized and quenched sample had Mo segregation, which is not the case. All the other pie charts in Figure 2 were constructed from data where PAGBs showed segregation of at least one of the five elements.

The main point of Figure 2 is to show that the degree and frequency of segregation and desegregation is extremely complex, depending on the steel and the specific stage of the heat treatment that has been completed. For example, in both steels, Ni segregation increases in both degree and frequency through all the four heat-treatment stages after which time ~90% of the PAGBs in steel #1 and > ~ 60% in steel #2 have Ni segregation. However, in steel #1, Mo, Cr, P and Mn desegregate during temper embrittlement, but increase in degree and frequency of segregation in steel #2. The temper-embrittlement process in steel #1, therefore, involves Mo de-segregation in agreement with previous

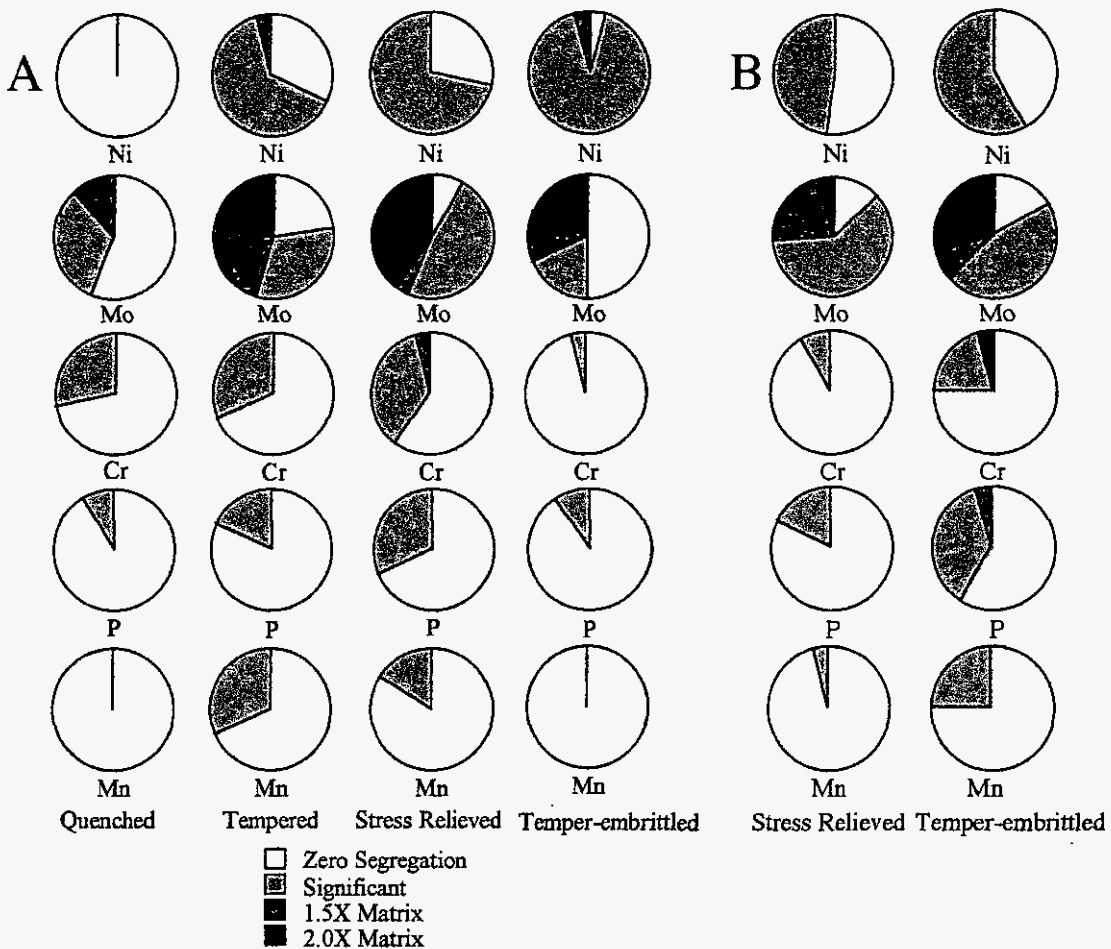


Figure 2. A) The five elemental pie charts for each of the four heat-treatment conditions for steel #1 and B) for the last two stages of heat treatment of steel #2.

Auger studies [6,7], but this is not a factor in steel #2. The behavior of P is intriguing given the general suspicion that it is a major player in temper embrittlement. It is important to be sure that the P K $\alpha$  X-ray peak is being clearly detected in the presence of the Mo L $\lambda$  peak as discussed in detail above. This apparent P desegregation in steel #1 mirrors the Cr and Mn behavior, not the Mo, which is strong evidence that any Mo/P peak overlap problem is not influencing the interpretation of the P line-profile data. This is less clear in steel #2 where the P and Mo trends are similar. However, more boundaries were detected with P segregation after temper embrittlement while the fraction of boundaries showing Mo segregation did not increase, only the degree of segregation. Therefore, it is concluded that the P segregation is correctly interpreted as increasing.

Previous work has shown [14,15] that “clean” and “super-clean” steel also temper-embrittle. A “clean” steel has the P content reduced to <0.01 wt%, while “super-clean” has both P and Mn reduced to ~0.003 and ~0.02 wt%, respectively. Therefore, the conclusion of this preliminary study is that temper-embrittlement is a function of segregation and desegregation of many elements. However, the results of this study, in combination with observations on clean and super-clean steels, indicate that segregation of Ni is of particular importance, in combination with the apparent desegregation of Mo, Cr, P and Mn in steel #1. Indeed, Freeman and co-workers [16,17,18] have shown, by ab-

initio calculations of site occupancy in pure Fe on the  $\Sigma_{111}^{re} 3$  boundary, that Mo enhances GB adhesion [16], whereas Ni slightly degrades it. However, earlier work by Freeman et al. [17,18] showed that P and Mn both embrittle the  $\Sigma_{111}^{re} 3$  boundary, but the largest embrittling effect is found when both Mn and P co-segregate as in steel #2. Therefore, the role of the individual elements, and particularly the effects of co-segregation need to be examined in more depth.

## CONCLUSIONS

In both steels:

- Ni starts to segregate to the PAGBs during tempering and continues to increase in degree and frequency through the subsequent heat treatments, particularly those in the temperature regime causing temper embrittlement.

In steel #1

- Mo segregates at all heat treatment stages then de-segregates strongly during temper-embrittlement.
- Cr segregation to the PAGBs remains approximately constant after austenitizing.
- P segregation starts during austenization and continues through tempering and stress relieving. During the temper-embrittling treatment, P de-segregates slightly.
- Mn segregates to the PAGBs during tempering, then de-segregates strongly during both the stress relief and temper-embrittlement treatments.
- Ni may play a hitherto unsuspected role in the temper embrittlement of this low-alloy steel.

In steel #2

- Mo, Cr, P and Mn all show increased frequency and degree of segregation during the temper embrittlement process.

A full understanding of segregation and desegregation behavior, therefore, requires that the PAGB chemistry be determined at each of the specific heat treatment steps.

## REFERENCES

- [1] M. Militzer, J. Wieting, *Acta Metall.* **37**, 10, 2585 (1989).
- [2] Y. Weng, C.J. McMahon, Jr., *Mat. Sci. Tech.* **3**, 207 (1987).
- [3] J.E. Wettig, A. Joshi, *Met. Trans. A* **21A**, 2817 (1990).
- [4] N. Bandyopadhyay, C.L. Briant, E.L. Hall, *Met. Trans. A*, **16A**, 721 (1985).
- [5] R.D.K. Misra, *Acta Metall.* **44**, 11, 4367 (1996).
- [6] C. J. McMahon, Jr., A. K. Cianelli and H.C. Feng, *Met. Trans. A* **8A**, 1055 (1977).
- [7] Z. Qu and C. J. McMahon, Jr., *Met. Trans. A* **14A** 1101 (1983).
- [8] V.V. Zabil'skii, *Metal Science and Heat Treatment*, **29**, 1, 32 (1987).
- [9] G. Pienaar, *Mat. Sci. Tech.* **2**, 1051 (1986).
- [10] A.J. Papworth, D.B. Williams, *Microscopy and Microanalysis, Proceedings*, **6** Supp. 2, 348 (2000).
- [11] A.J. Papworth, D.B. Williams, *Scripta Materialia*, **42**, 627 (2000).
- [12] A.J. Papworth, D.B. Williams, *Scripta Materialia*, **42**, 1107 (2000).
- [13] A.J. Papworth, M. Watanabe and D.B. Williams *Ultramicroscopy*, **88**, 265 (2001).
- [14] G. Thauvin, G. Lorang, C. Leymonie, *Met. Trans. A* **23A**, 2243 (1992).
- [15] J. Nutting, *Ironmaking and Steelmaking*, **16**, 4, 219 (1989).
- [16] W.T. Geng, A.J. Freeman, R. Wu, G.B. Olson, *Phys. Rev. B* **62**, 10, 6208 (2000).
- [17] L. Zhong, R. Wu, A.J. Freeman, G.B. Olson, *Phys. Rev. B* **55**, 17, 11133 (1997).
- [18] R. Wu, A.J. Freeman, G.B. Olson, *Phys. Rev. B* **50**, 1, 75 (1994).